

Washington University School of Medicine

Digital Commons@Becker

---

2020-Current year OA Pubs

Open Access Publications

---

2-9-2023

## The mechanism of enantioselective neurosteroid actions on GABA

Hiroki Tateiwa

*Washington University School of Medicine in St. Louis*

Satyanarayana M Chintala

*Washington University School of Medicine in St. Louis*

Ziwei Chen

*Washington University School of Medicine in St. Louis*

Lei Wang

*Washington University School of Medicine in St. Louis*

Fatima Amtashar

*Washington University School of Medicine in St. Louis*

*See next page for additional authors*

Follow this and additional works at: [https://digitalcommons.wustl.edu/oa\\_4](https://digitalcommons.wustl.edu/oa_4)

 Part of the [Medicine and Health Sciences Commons](#)

Please let us know how this document benefits you.

---

### Recommended Citation

Tateiwa, Hiroki; Chintala, Satyanarayana M; Chen, Ziwei; Wang, Lei; Amtashar, Fatima; Bracamontes, John; Germann, Allison L; Pierce, Spencer R; Covey, Douglas F; Akk, Gustav; and Evers, Alex S, "The mechanism of enantioselective neurosteroid actions on GABA." *Biomolecules*. 13, 2. 341 (2023).

[https://digitalcommons.wustl.edu/oa\\_4/1905](https://digitalcommons.wustl.edu/oa_4/1905)

This Open Access Publication is brought to you for free and open access by the Open Access Publications at Digital Commons@Becker. It has been accepted for inclusion in 2020-Current year OA Pubs by an authorized administrator of Digital Commons@Becker. For more information, please contact [vanam@wustl.edu](mailto:vanam@wustl.edu).



---

**Authors**

Hiroki Tateiwa, Satyanarayana M Chintala, Ziwei Chen, Lei Wang, Fatima Amtashar, John Bracamontes, Allison L Germann, Spencer R Pierce, Douglas F Covey, Gustav Akk, and Alex S Evers

## Article

# The Mechanism of Enantioselective Neurosteroid Actions on GABA<sub>A</sub> Receptors

Hiroki Tateiwa<sup>1,2</sup>, Satyanarayana M. Chintala<sup>1</sup> , Ziwei Chen<sup>1,3</sup>, Lei Wang<sup>1,4</sup> , Fatima Amtashar<sup>1</sup>, John Bracamontes<sup>1</sup>, Allison L. Germann<sup>1</sup>, Spencer R. Pierce<sup>1</sup>, Douglas F. Covey<sup>1,3,5,6</sup>, Gustav Akk<sup>1,3</sup> and Alex S. Evers<sup>1,3,6,\*</sup> 

<sup>1</sup> Department of Anesthesiology, Washington University School of Medicine, St. Louis, MO 63110, USA

<sup>2</sup> Department of Anesthesiology and Intensive Care Medicine, Kochi Medical School, Kochi 7838505, Japan

<sup>3</sup> Taylor Institute for Innovative Psychiatric Research, St. Louis, MO 63110, USA

<sup>4</sup> Department of Anesthesiology, Union Hospital, Tongji Medical College, Huazhong University of Sciences and Technology, Wuhan 430074, China

<sup>5</sup> Department of Psychiatry, Washington University School of Medicine, St. Louis, MO 63110, USA

<sup>6</sup> Department of Developmental Biology (Pharmacology), Washington University School of Medicine, St. Louis, MO 63110, USA

\* Correspondence: eversa@wustl.edu; Tel.: +1-314-362-8557

**Abstract:** The neurosteroid allopregnanolone (ALLO) and pregnanolone (PREG), are equally effective positive allosteric modulators (PAMs) of GABA<sub>A</sub> receptors. Interestingly, the PAM effects of ALLO are strongly enantioselective, whereas those of PREG are not. This study was aimed at determining the basis for this difference in enantioselectivity. The oocyte electrophysiology studies showed that *ent*-ALLO potentiates GABA-elicited currents in  $\alpha_1\beta_3$  GABA<sub>A</sub> receptors with lower potency and efficacy than ALLO, PREG or *ent*-PREG. The small PAM effect of *ent*-ALLO was prevented by the  $\alpha_1$ (Q242L) mutation in the intersubunit neurosteroid binding site between the  $\beta_3$  and  $\alpha_1$  subunits. Consistent with this result, neurosteroid analogue photolabeling with mass spectrometric readout, showed that *ent*-ALLO binds weakly to the  $\beta_3$ - $\alpha_1$  intersubunit binding site in comparison to ALLO, PREG and *ent*-PREG. Rigid body docking predicted that *ent*-ALLO binds in the intersubunit site with a preferred orientation 180° different than ALLO, PREG or *ent*-PREG, potentially explaining its weak binding and effect. Photolabeling studies did not identify differences between ALLO and *ent*-ALLO binding to the  $\alpha_1$  or  $\beta_3$  intrasubunit binding sites that also mediate neurosteroid modulation of GABA<sub>A</sub> receptors. The results demonstrate that differential binding of *ent*-ALLO and *ent*-PREG to the  $\beta_3$ - $\alpha_1$  intersubunit site accounts for the difference in enantioselectivity between ALLO and PREG.

**Keywords:** neurosteroids; GABA-A receptors; enantiomers; photolabeling



**Citation:** Tateiwa, H.; Chintala, S.M.; Chen, Z.; Wang, L.; Amtashar, F.; Bracamontes, J.; Germann, A.L.; Pierce, S.R.; Covey, D.F.; Akk, G.; et al. The Mechanism of Enantioselective Neurosteroid Actions on GABA<sub>A</sub> Receptors. *Biomolecules* **2023**, *13*, 341. <https://doi.org/10.3390/biom13020341>

Academic Editor: Katarina Vukojević

Received: 11 January 2023

Revised: 30 January 2023

Accepted: 7 February 2023

Published: 9 February 2023



**Copyright:** © 2023 by the authors. Licensee MDPI, Basel, Switzerland. This article is an open access article distributed under the terms and conditions of the Creative Commons Attribution (CC BY) license (<https://creativecommons.org/licenses/by/4.0/>).

## 1. Introduction

Enantiomers are molecules with opposite stereochemistry at every chiral center. They have identical physical properties, but have non-superimposable mirror image structures and rotate polarized light in opposite directions. Enantiomers of hydrophobic ligands have equal solubility in lipids and are equally effective at disrupting lipid bilayers [1–3]. Enantioselectivity has thus been used as a criterion for demonstrating that a hydrophobic ligand modulates membrane protein activity by interacting with specific chiral protein binding sites rather than by perturbing membrane properties [2,4].

The demonstration that the anesthetic neurosteroid allopregnanolone (3 $\alpha$ -hydroxy-5 $\alpha$ -pregnan-20-one ALLO) is an enantioselective modulator of GABA<sub>A</sub> receptor currents and an enantiospecific anesthetic provided the initial evidence that neurosteroids bind to specific sites on GABA<sub>A</sub> receptors to enhance GABA currents and produce anesthesia [5,6]. Pregnanolone (3 $\alpha$ -hydroxy-5 $\beta$ -pregnan-20-one; PREG), the 5 $\beta$ -epimer of ALLO, is also

a positive allosteric modulator of GABA<sub>A</sub> currents and an anesthetic, but has minimal enantioselectivity either as a modulator of GABA<sub>A</sub> receptors or as an anesthetic [7].

It has subsequently been shown using site-directed mutagenesis [8], neurosteroid analogue photoaffinity labeling [9–11] and x-ray crystallography [12–14] that PAM neurosteroids bind in an intersubunit site between the third transmembrane helix (TM3) of a GABA<sub>A</sub>  $\beta$ -subunit and the first transmembrane helix (TM1) of an adjacent  $\alpha$ -subunit. Occupancy of this site is the major contributor to the PAM effect of neurosteroids and mutations to the Q242 and W246 residues in this site largely ablate PAM activity [8,15–17]. Photoaffinity labeling studies have shown that PAM neurosteroid binding to intrasubunit sites in the  $\alpha$ -subunit (between TM1 and TM4) and the  $\beta$ -subunit (between TM3 and TM4) also contributes to modulation of GABA<sub>A</sub> receptors [9,15,16,18].

To determine the molecular mechanism underlying the differential enantioselective effects of ALLO and PREG, we examined the binding of ALLO, PREG and their enantiomers (*ent*-ALLO and *ent*-PREG) to the three neurosteroid binding sites on  $\alpha_1\beta_3$  GABA<sub>A</sub> receptors. Site-specific binding was determined by measuring the ability of the PAM neurosteroids and their enantiomers to prevent neurosteroid analogue photolabeling of peptides in each of the binding sites. We also used KK152, the enantiomer of the ALLO-analogue photolabeling reagent KK123, to confirm enantiomer binding to the intrasubunit sites. The binding results were correlated with electrophysiological studies examining the effects of the PAM neurosteroids and their enantiomers on GABA<sub>A</sub> currents in wild type receptors and in receptors with an  $\alpha_1$ (Q242L) mutation in the intersubunit binding site. Collectively, the experimental data demonstrate that the difference in enantioselectivity between ALLO and PREG results from the differential binding of *ent*-ALLO and *ent*-PREG in the canonical  $\beta_3$ - $\alpha_1$  intersubunit binding site. The structural basis for this difference was explored using rigid body molecular docking.

## 2. Materials and Methods

### 2.1. Receptor Expression in *Xenopus laevis* Oocytes and Electrophysiological Recordings

GABA<sub>A</sub> receptors were expressed in oocytes from the African clawed frog (*X. laevis*). The oocytes were purchased as quarter ovaries from Xenopus1 (Dexter, MI, USA). The ovaries were digested in a 2% *w/v* (mg/mL) solution of collagenase A in ND96 solution (96 mM NaCl, 2 mM KCl, 1.8 mM CaCl<sub>2</sub>, 1 mM MgCl<sub>2</sub>, 5 mM HEPES; pH 7.4) containing 100 U/mL penicillin and 100  $\mu$ g/mL streptomycin for 30 to 40 min at 37 °C.

The cDNAs containing the human  $\alpha_1$  or  $\beta_3$  subunits were linearized with XbaI (NEB Labs, Ipswich, MA, USA), and the cRNAs were generated using T7 mMessage mMachine (Ambion, Austin, TX, USA). The  $\alpha_1$ (Q242L) and  $\alpha_1$ (V227W) mutations were generated using the QuikChange Site-Directed Mutagenesis Kit (Agilent Technologies, Santa Clara, CA, USA), and the coding region was fully sequenced prior to use. The functional properties of the  $\alpha_1$ (Q242L) and  $\alpha_1$ (V227W) mutants have been reported in previous publications [8,9,16,17]. The oocytes were injected with a total of 12 ng cRNA. The ratio of cRNAs was 5:1 ( $\alpha_1$ : $\beta_3$ ) to minimize the expression of  $\beta_3$  homomeric receptors. Following injection, the oocytes were incubated in ND96 at 16 °C for 2 days prior to conducting electrophysiological recordings.

Electrophysiological recordings were conducted using standard two-electrode voltage clamp. Borosilicate capillary glass tubing (G120F-4, OD = 1.20 mm, ID = 0.69 mm; Warner Instruments, Hamden, CT, USA) was used for voltage and current electrodes. The electrodes were filled with 3 M KCl and had resistances of 0.3–1 M $\Omega$ . The oocytes were clamped at –60 mV. The chamber (RC-1Z; Warner Instruments) was perfused with ND96 at 5–8 mL min<sup>–1</sup>. Solutions were gravity-applied from 30-mL glass syringes with glass luer slips via Teflon tubing, to minimize drug absorption. The current responses were amplified with an OC-725C amplifier (Warner Instruments), digitized with a Digidata 1200 series digitizer (Molecular Devices, San Jose, CA, USA) and stored using pClamp (Molecular Devices). The peak amplitude was determined using Clampfit (Molecular Devices). The stock solution of GABA was made in ND96 bath solution at 500 mM, stored in aliquots at

−20 °C, and diluted as needed on the day of experiment. Activation by steroids was tested by co-applying a steroid with 0.2–0.5 μM GABA for wild type receptors (Figure 1B,C) and 0.5–3.0 μM GABA for the α<sub>1</sub>(Q242L)β<sub>3</sub> receptors (Figure 1E) to achieve a target probability of being in the active state (P<sub>A</sub>) of 0.05–0.1. For steroid concentration-response curves (Figure 1D), steroid was co-applied with 0.8–3 μM GABA to achieve a target P<sub>A</sub> of ~0.2. The steroids were dissolved in DMSO at 10 mM and stored at room temperature.

The effects of steroids were estimated by calculating the ratio of the peak responses to GABA + steroid and GABA alone. Descriptive analysis of steroid-potential was carried out by fitting the steroid concentration-response data to the Hill equation. Mechanistic analysis of steroid-potential was conducted in the framework of a cyclic two-state (Resting-Active) concerted transition model [19,20]. In brief, the raw current amplitudes were converted to units of P<sub>A</sub> by normalizing the responses to GABA or GABA + steroid to the response to 1 mM GABA + 50 μM propofol that was considered to generate a response with peak P<sub>A</sub> of ~1 [21]. The concentration response data were then fitted to the state function:

$$P_A = \frac{1}{1 + L * \left[ \frac{1 + [\text{steroid}]/K_{R,\text{steroid}}}{1 + [\text{steroid}]/(K_{R,\text{steroid}} c_{\text{steroid}})} \right]^{N_{\text{steroid}}}} \quad (1)$$

where L\* is the P<sub>A</sub> of the response to GABA alone in the same cell and is calculated as (1 − P<sub>A,GABA</sub>)/P<sub>A,GABA</sub>, [steroid] is the concentration of steroid, K<sub>R,steroid</sub> is the equilibrium dissociation constant of the steroid in the resting receptor, c<sub>steroid</sub> is the ratio of the equilibrium dissociation constant in the active receptor to K<sub>R,steroid</sub>, and N<sub>steroid</sub> is the number of steroid binding sites (by convention, constrained to 2). A higher value of c<sub>steroid</sub> indicates lower efficacy. Free energy change provided by the steroid can be calculated as ΔG = NRT × ln(c<sub>steroid</sub>). The curve-fitting was carried out using Origin 2020 (OriginLab Corp, Northampton, MA, USA). The data are presented as mean ± SD.

## 2.2. Cell Culture, Protein Expression and Membrane Preparation

A tetracycline-inducible cell line expressing human α<sub>1</sub>-8xHis-FLAG and human β<sub>3</sub> GABA<sub>A</sub> receptor subunits in HEK-T-Rex<sup>TM</sup>-293 cells was generated and propagated as previously described [9]. Briefly, stably transfected cells were cultured under the following conditions: cells were maintained in DMEM/F-12 50/50 medium containing 10% fetal bovine serum (tetracycline-free, Takara, Mountain View, CA, USA), penicillin (100 units/mL), streptomycin (100 g/mL), blasticidin (2 mg/mL), hygromycin (50 μg/mL) and zeocin (20 μg/mL) at 37 °C in a humidified atmosphere containing 5% CO<sub>2</sub>. Cells were passaged twice each week, maintaining subconfluent cultures. For protein production, cells were plated into dishes. When the cells reached 50% confluence, GABA receptor expression was induced with 1 μg/mL doxycycline with the addition of 5 mM sodium butyrate and the cells were grown to confluence. 48 to 72 h after induction the cells were harvested and washed twice with a buffer containing 10 mM potassium phosphate, 100 mM potassium chloride (pH 7.5) plus protease inhibitors (Sigma-Aldrich, St. Louis, MO, USA). Cells were collected by centrifugation at 1000× g at 4 °C for 5 min and homogenized with a glass mortar and a Teflon pestle for ten strokes on ice. Membranes were collected by centrifugation at 40,000× g at 4 °C for 30 min and resuspended in a buffer containing 10 mM potassium phosphate, 100 mM potassium chloride (pH 7.5). Protein concentration was determined with micro-BCA protein assay (Thermo Fisher Scientific, Waltham, MA, USA). GABA<sub>A</sub> receptor content of the membranes was determined by measuring the B<sub>max</sub> of [<sup>3</sup>H]muscimol binding as previously described [9] and assuming that each mole of receptor contains two muscimol binding sites. Membranes were stored at −80 °C.

## 2.3. Photolabeling and Purification of α<sub>1</sub>β<sub>3</sub> GABA<sub>A</sub>R

The syntheses of the neurosteroid photolabeling reagents KK123, KK152 and KK200 are detailed in previous reports [22,23]. For each photolabeling experiment, 10–20 mg of HEK cell membrane protein containing 100–150 pmoles of α<sub>1</sub>β<sub>3</sub> GABA<sub>A</sub> receptor was used.

Frozen membranes were thawed and resuspended at a final concentration of  $1.25 \text{ mg ml}^{-1}$  in a buffer containing 10 mM potassium phosphate, 100 mM potassium chloride (pH 7.5), and 1 mM GABA. For the photolabeling competition experiments, 3  $\mu\text{M}$  KK123 or KK200 in the presence of 30  $\mu\text{M}$  competitor (ALLO, *ent*-ALLO, PREG, and *ent*-PREG), or the same volume of ethanol for control group, was added to the membrane suspension and incubated on ice for 1 h. The samples were then irradiated in a quartz cuvette for 5 min, using a photoreactor emitting light with wavelengths  $>320 \text{ nm}$  [24]. Membranes were then collected by centrifugation at  $20,000 \times g$  at  $4 \text{ }^\circ\text{C}$  for 30 min. The photolabeled membrane proteins were resuspended in lysis buffer containing 1% n-dodecyl- $\beta$ -D-maltoside (DDM) (Anatrace, Maumee, OH, USA), 0.25% cholesteryl hemisuccinate (CHS) (Anatrace, Maumee, OH, USA), 50 mM Tris (pH 7.5), 150 mM NaCl, 2 mM  $\text{CaCl}_2$ , 5 mM KCl, 5 mM  $\text{MgCl}_2$ , 1 mM EDTA, 10% glycerol at a final concentration of  $1 \text{ mg ml}^{-1}$ . The membrane protein suspension was homogenized using a glass mortar and a Teflon pestle and incubated at  $4 \text{ }^\circ\text{C}$  overnight. The protein lysate was centrifuged at  $15,000 \times g$  at  $4 \text{ }^\circ\text{C}$  for 30 min and the supernatant was incubated with 0.5 mL anti-FLAG agarose (Sigma-Aldrich, St. Louis, MO, USA) at  $4 \text{ }^\circ\text{C}$  for 2 h. The anti-FLAG agarose was then transferred to an empty column, followed by washing with 20 mL of washing buffer (50 mM triethylammonium bicarbonate and 0.02% DDM). GABA<sub>A</sub> receptors were eluted with aliquots of  $200 \mu\text{g ml}^{-1}$  FLAG tag peptide and  $100 \mu\text{g ml}^{-1}$  3X FLAG (ApexBio) in the washing buffer. Pooled eluates (4 mL) containing GABA<sub>A</sub> receptors were concentrated to 100  $\mu\text{L}$  using 100 kDa cut-off centrifugal filters.

#### 2.4. Middle-Down MS Analysis

The purified  $\alpha_1\beta_3$  GABA<sub>A</sub> receptors (100  $\mu\text{L}$ ) were reduced with 5 mM tris(2-carboxyethyl) phosphine for 30 min, followed by alkylation with 5 mM N-ethylmaleimide (NEM) for 45 min in the dark. The NEM was quenched with 5 mM dithiothreitol (DTT) for 15 min. These three steps were carried out at room temperature. Samples were then digested with 8  $\mu\text{g}$  of trypsin for 7 days at  $4 \text{ }^\circ\text{C}$  to obtain maximal recovery of TMD peptides. The digestions were terminated by adding formic acid to a final concentration of 1%, followed directly by LC-MS analysis on an Orbitrap Elite mass spectrometer. 20  $\mu\text{L}$  samples were injected into a home-packed PLRP-S (Agilent, Santa Clara, CA, USA) column (10 cm  $\times$  75  $\mu\text{m}$ , 300  $\text{\AA}$ ), separated with a 135 min gradient from 10% to 90% acetonitrile, and introduced to the mass spectrometer at  $800 \text{ nL min}^{-1}$  with a nanospray source. MS acquisition was set as a MS1 Orbitrap scan (resolution of 60,000) followed by top 20 MS2 Orbitrap scans (resolution of 15,000) using data-dependent acquisition, and exclusion of singly charged precursors. Fragmentation was performed using high-energy dissociation with normalized energy of 35%. Analysis of datasets was performed using Xcalibur (Thermo Fisher Scientific) to manually search for TM1, TM2, TM3 or TM4 tryptic peptides with or without neurosteroid photolabeling modifications. Photolabeling efficiency was estimated by generating extracted chromatograms of unlabeled and labeled peptides, determining the area under the curve, and calculating the abundance of labeled peptide/(unlabeled + labeled peptide). Analysis of statistical significance comparing the photolabeling efficiency of KK123 and KK200 for  $\alpha_1\beta_3$  GABA<sub>A</sub>R was determined using one-way ANOVA with Bonferroni's multiple comparisons test (GraphPad Prism version 9.4.0 for Windows, GraphPad Software, San Diego, CA, USA). MS2 spectra of photolabeled TMD peptides were analyzed by manual assignment of fragment ions with and without photolabeling modification. Fragment ions were accepted based on the presence of a monoisotopic mass within 20 ppm mass accuracy. In addition to manual analysis, PEAKS (Bioinformatics Solutions Inc., Waterloo, ON, Canada) database searches were performed for datasets of photolabeled  $\alpha_1\beta_3$  GABA<sub>A</sub>R. Search parameters were set for a precursor mass accuracy of 20 ppm, fragment ion accuracy of 0.1 Da, up to three missed cleavages on either end of the peptide, false discovery rate of 0.1%, and variable modifications of methionine oxidation, cysteine alkylation with NEM and DTT, and neurosteroid analogue photolabeling reagents on any amino acid.



### 2.5. Molecular Docking and Binding Energy Calculations

The molecular coordinates of ALLO (PubChem CID: 92786) and PREG (PubChem CID: 31402) were obtained from PubChem. The structures of *ent*-ALLO and *ent*-PREG were generated by inverting the chiral configurations of all the chiral centers in the structures of ALLO and PREG. These structures were then energy minimized using UFF force field and Steepest Descent algorithm in the Avogadro software [25] to obtain the coordinates of *ent*-ALLO and *ent*-PREG. The docking template of  $\alpha_1\beta_3\gamma_2$  was generated using the CryoEM structure (PDB: 6HUO) [26]. The ligands bound to the protein were deleted and the structure was energy minimized in Chimera ver. 1.16 [27]. DockPrep was used to add hydrogens and charges to the protein structure. The interface between  $\beta_3$ -TM3 and  $\alpha_1$ -TM1 was used for grid generation of size  $20 \times 18 \times 29 \text{ \AA}$  encompassing the neurosteroid binding site. Docking was performed using AutoDock Vina [28] in the Chimera software to obtain the binding energies and binding poses of ALLO, PREG, *ent*-ALLO and *ent*-PREG.

## 3. Results

### 3.1. Potentiation of $\alpha_1\beta_3$ GABA<sub>A</sub> Currents by Enantiomeric Neurosteroids

We initially examined the effects of ALLO, *ent*-ALLO, PREG and *ent*-PREG (Figure 1A) on GABA-elicited currents in wild-type  $\alpha_1\beta_3$  GABA<sub>A</sub> receptors expressed in *Xenopus* oocytes. Representative traces (Figure 1B) illustrate that 10  $\mu\text{M}$  concentrations of each of the steroids potentiate the currents elicited by low (0.2–0.5  $\mu\text{M}$ ;  $P_A = 0.06 \pm 0.03$ ; mean  $\pm$  S.D. from 48 cells) GABA. Quantitative analysis (Figure 1C) shows that 10  $\mu\text{M}$  ALLO, PREG and *ent*-PREG enhance GABA-elicited currents to a similar extent ( $p > 0.05$ ). In contrast, *ent*-ALLO enhances GABA-elicited currents to a lesser extent than any of the other steroids ( $p < 0.001$  vs. ALLO, PREG and *ent*-PREG).

Concentration-response curves (Figure 1D) comparing the potentiation of GABA-elicited currents (GABA = 0.8–3  $\mu\text{M}$ ; target  $P_A = 0.2$ ) indicate lower apparent potency for *ent*-ALLO ( $EC_{50} = 2.00 \pm 0.30 \mu\text{M}$ ;  $n = 5$ ) than ALLO ( $EC_{50} = 0.08 \pm 0.01 \mu\text{M}$ ;  $n = 5$ ). Fitting the data from Figure 1D to Equation (1) yielded  $K_{R,steroid}$  values of  $0.22 \pm 0.19$  and  $2.39 \pm 1.17 \mu\text{M}$  and  $c_{steroid}$  values of  $0.199 \pm 0.053$  and  $0.561 \pm 0.065$  for ALLO and *ent*-ALLO, respectively, indicating that *ent*-ALLO is both less potent and less efficacious than ALLO.

To determine whether the modest PAM effect of *ent*-ALLO is mediated by the  $\beta_3/\alpha_1$  intersubunit binding site, we next examined the effects of the neurosteroid enantiomeric pairs in receptors with an  $\alpha_1$ (Q242L) mutation in the intersubunit site. The enhancement of GABA<sub>A</sub> currents by ALLO, PREG and their enantiomers was eliminated in  $\alpha_1$ (Q242L) $\beta_3$  receptors. This is quantitatively illustrated in Figure 1E, which shows the ratio of the effect of a 10  $\mu\text{M}$  concentration of each steroid to the baseline GABA response. These data indicate that while *ent*-ALLO is a weak allosteric agonist, its PAM effect is still predominantly mediated by the canonical  $\beta_3/\alpha_1$  intersubunit binding site.

PAM actions of steroids are additionally mediated by the  $\alpha_1$ -intrasubunit site [9,16]. To confirm the lower efficacy of *ent*-ALLO at the  $\beta_3/\alpha_1$  intersubunit site, we compared the effects of 10  $\mu\text{M}$  ALLO and *ent*-ALLO on currents elicited by GABA ( $P_A < 0.1$ ) in receptors in which the actions of steroids in the  $\alpha_1$ -intrasubunit site are prevented by the  $\alpha_1$ (V227W) mutation. In the  $\alpha_1$ (V227W) $\beta_3$  receptor, application of ALLO potentiated the response to GABA to  $321 \pm 65\%$  ( $n = 5$ ) of control while application of *ent*-ALLO potentiated to only  $135 \pm 41\%$  ( $n = 5$ ) of control (Figure 1F). These data confirm that the difference in efficacy between ALLO and *ent*-ALLO acting at the  $\beta_3/\alpha_1$  intersubunit binding site accounts for the enantioselective PAM effect of ALLO. We note that the effects of mutations to the  $\beta_3/\alpha_1$  intersubunit site and the  $\alpha_1$ -intrasubunit site ( $\alpha_1$ (Q242L) and  $\alpha_1$ (V227W), respectively) are not strictly additive, indicating that the two sites are allosterically linked in the  $\alpha_1\beta_3$  receptor.

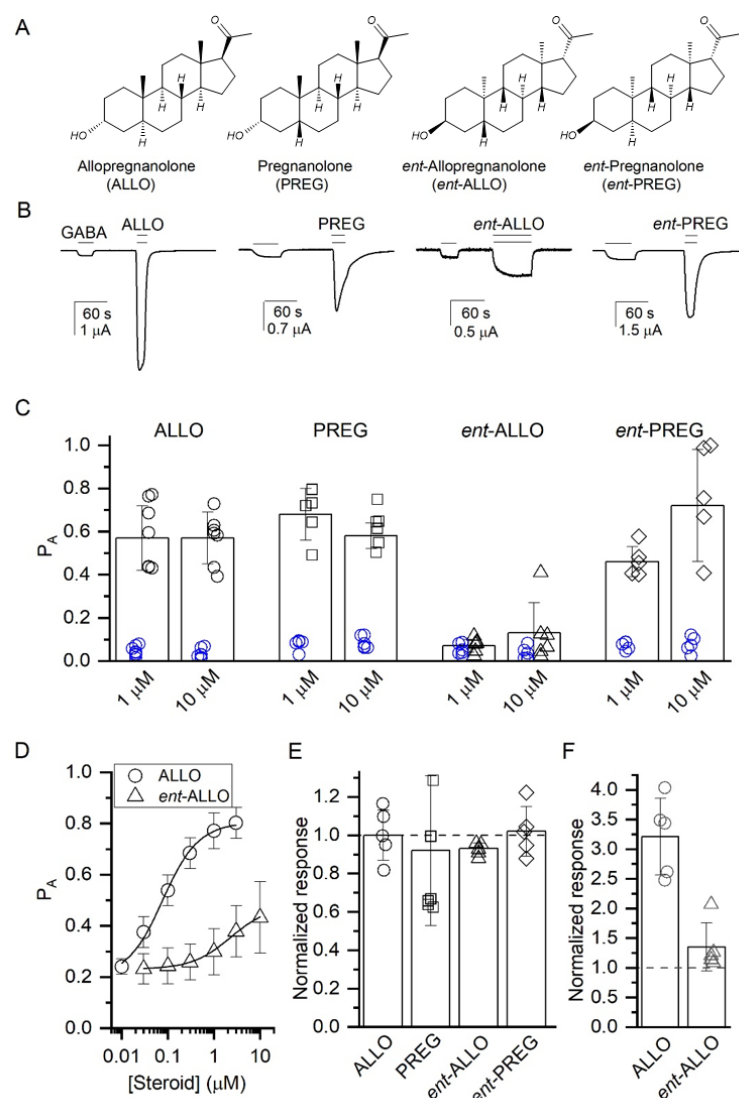


**Figure 1.** Effects of ALLO, PREG, *ent*-ALLO and *ent*-PREG on GABA-elicited currents in  $\alpha_1\beta_3$  GABA<sub>A</sub> receptors expressed in *Xenopus* oocytes. (A) Steroid structures (B) Representative traces of currents elicited by low GABA (0.2–0.5  $\mu$ M;  $P_A = 0.06 \pm 0.03$ ) in the presence or absence of 10  $\mu$ M concentrations of steroids. (C) Enhancement of currents elicited with low GABA ( $n = 5$ ) by 1 and 10  $\mu$ M steroids. Blue symbols indicate response with GABA alone and black symbols are for GABA + steroid. Open probabilities for steroid-enhanced currents at 1 and 10  $\mu$ M were compared using one way ANOVA. There was a statistically significant difference between groups as determined by one-way ANOVA ( $F(3,20) = 33.29$ ,  $p < 0.001$  for 1  $\mu$ M;  $F(3,20) = 18.45$ ,  $p < 0.001$  for 10  $\mu$ M). A Bonferroni post-hoc multiple comparison test of the means revealed that at both 1 and 10  $\mu$ M the effect of *ent*-ALLO was significantly different compared to the effects of ALLO, PREG, and *ent*-PREG ( $p < 0.001$  for each comparison). (D) Concentration-response curves comparing potentiation of GABA-elicited currents (GABA = 0.8–3  $\mu$ M; target  $P_A = 0.2$ ) by ALLO and *ent*-ALLO. Fitting to an MWC model (Equation (1)) indicates that *ent*-ALLO is both less potent than ALLO ( $K_{R,steroid}$  values of  $0.22 \pm 0.19$  and  $2.39 \pm 1.17$   $\mu$ M, respectively) and less efficacious ( $c$  values of  $0.199 \pm 0.053$  and  $0.561 \pm 0.065$ , respectively). (E) Potentiation of GABA (target  $P_A = 0.06$ ) by ALLO, *ent*-ALLO, PREG and *ent*-PREG in  $\alpha_1(Q242L)\beta_3$  receptors. The data indicate that potentiation of GABA responses by all of the steroids is eliminated by a mutation in the intersubunit site. (F) Potentiation of GABA ( $P_A < 0.1$ ) by ALLO and *ent*-ALLO (10  $\mu$ M) in  $\alpha_1(V227W)\beta_3$  receptors. The difference in efficacy between ALLO and *ent*-ALLO is preserved in the V227 W mutant. Figures (E,F) show the ratio of the response to GABA + steroid to GABA alone, with a ratio of 1 indicating no steroid response.



### 3.2. Competitive Prevention of Labeling with ALLO-Analogue Photolabeling Reagents

To directly determine whether ALLO, PREG and their enantiomers bind to each of the neurosteroid binding sites on  $\alpha_1\beta_3$  GABA<sub>A</sub> receptors, we measured their ability to prevent neurosteroid-analogue photolabeling of peptides in each of these sites. It has previously been shown that the ALLO-analogue photolabeling reagent, KK200 (Figure 2A), labels residue G308 at the cytoplasmic end of  $\beta_3$  TM3 in the interface between the  $\beta_3$  and  $\alpha_1$  subunits (Figure 2B and Figure S1). [9]. The ability of each neurosteroid to prevent photolabeling of G308 by 3  $\mu$ M KK200 was used to assay binding to the  $\beta_3/\alpha_1$  intersubunit site. 30  $\mu$ M ALLO, PREG and *ent*-PREG completely prevented KK200 labeling of the  $\beta_3$  TM3 peptide ( $p < 0.001$  vs. control), whereas 30  $\mu$ M *ent*-ALLO partially, but not significantly ( $p = 0.06$ , control vs. 30  $\mu$ M *ent*-AlloP), reduced labeling. 10  $\mu$ M ALLO also completely inhibited KK200 labeling of G308, whereas 10  $\mu$ M *ent*-ALLO did not inhibit labeling, confirming that ALLO binds enantioselectively in the intersubunit site (Figure 2C). While there was no significant difference between the photolabeling efficiency of the control and the 10 or 30  $\mu$ M *ent*-ALLO samples, the trend toward reduced labeling with increasing concentrations of *ent*-ALLO suggests that it binds to the intersubunit site with very low affinity. Of note, KK200 also labels the  $\alpha_1$  intrasubunit site at residue N408 on  $\alpha_1$ -TM4, but the efficiency of labeling was insufficient to measure competitive prevention of photolabeling.

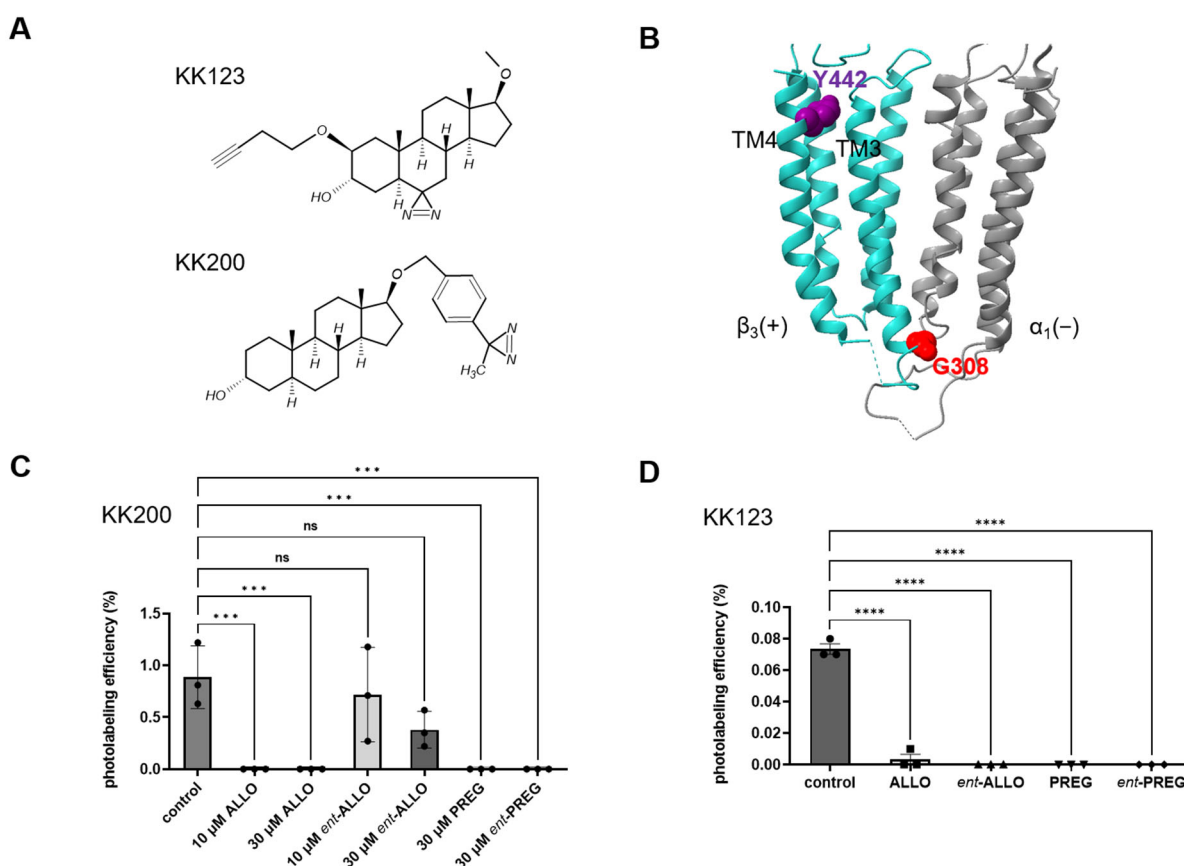


**Figure 2.** Competitive inhibition of neurosteroid analogue photolabeling. (A) Structures of the neurosteroid analogue photolabeling reagents KK200 and KK123. (B) Structure of the  $\alpha_1\beta_3$  GABA<sub>A</sub> receptor transmembrane domains highlighting residue Y442 on  $\beta_3$ -TM4 (purple) which is labeled by KK123 and residue G308 on  $\beta_3$ -TM3 (red) which is labeled by KK200. The  $\alpha_1$  subunit is shown in grey and the  $\beta_3$  subunit in turquoise. (C) photolabeling efficiency of  $\beta_3$  subunit TM3 by 3  $\mu$ M KK200 in  $\alpha_1\beta_3$  GABA<sub>A</sub> receptors in the absence (control) or presence of either 10 or 30  $\mu$ M allopregnanolone (ALLO), *ent*-allopregnanolone (*ent*-ALLO), pregnanolone (PREG) or *ent*-pregnanolone (*ent*-PREG). There was a statistically significant difference between groups as determined by one-way ANOVA

( $F(6, 14) = 9.393, p < 0.001$ ). Bonferroni's post-hoc multiple comparison test of the means showed that the effects of ALLO, PREG, and *ent*-PREG were all significantly different than control ( $p < 0.001$  vs. control for each comparison) whereas the effects of *ent*-ALLO were not significantly different than control ( $p = 0.85$  for control vs.  $10 \mu\text{M}$  *ent*-ALLO and  $p = 0.06$  for control vs.  $30 \mu\text{M}$  *ent*-ALLO). (D) Photolabeling efficiency of  $\beta_3$  subunit TM4 by  $3 \mu\text{M}$  KK123 in  $\alpha_1\beta_3$  GABA<sub>A</sub> receptors in the absence (control) or presence of  $30 \mu\text{M}$  competitive steroid. There was a statistically significant difference between groups as determined by one-way ANOVA  $F(4, 10) = 237.0, p < 0.0001$ . Bonferroni's post-hoc multiple comparison test of the means showed that the effects of ALLO, PREG, *ent*-ALLO and *ent*-PREG were all significantly different than control ( $p < 0.0001$  vs. control for each comparison) In Panels C and D data are shown as mean  $\pm$  range with  $n = 3$  for each point. Statistical differences: \*\*\* =  $p < 0.001$ ; \*\*\*\* =  $p < 0.0001$ ; ns = not significant.

### 3.3. Docking Simulation

To probe the structural basis for the reduced binding of *ent*-ALLO to the intersubunit site, rigid body docking of ALLO, *ent*-ALLO, PREG and *ent*-PREG to the  $\beta_3/\alpha_1$  intersubunit site was analyzed using a cryo-EM structure (PDB: 6HUO) of an  $\alpha_1\beta_3\gamma_2$  GABA<sub>A</sub> receptor [26]. The neurosteroids docked between  $\beta_3$ -TM3 and  $\alpha_1$ -TM1 in poses with two distinct orientations: (1) poses in which the steroid 3-hydroxy group is proximal to the Q242 residue on  $\alpha_1$ -TM1 and the 17-methyl ketone is proximal to F301 on  $\beta_3$ -TM3 (orientation #1) or; (2) poses in which the 3-hydroxy group is proximal to F301 on  $\beta_3$ -TM3 and the 17-methyl ketone is near Q242 on  $\alpha_1$ TM1 (orientation #2). For ALLO, the lowest energy pose is in orientation #1 with the 18 and 19 methyl groups both pointing to the lipid surface of  $\beta_3$ -TM3 (Figure 3A). This is the same pose observed in the X-ray structures of THDOC bound to the GLIC- $\alpha_1$ GABA<sub>A</sub> chimera [13] and alphaxalone bound to the ELIC- $\alpha_1$ GABA<sub>A</sub> chimera [14]. ALLO was also observed in poses with orientation #2, but with significantly less negative binding energy (Table 1). The energetically preferred docking pose for PREG is also in orientation #1 and is almost identical to the pose observed in the crystal structure of PREG bound to the  $\beta_3/\alpha_5$  chimeric GABA<sub>A</sub> receptor [12] (Figure 3a). In the preferred poses of ALLO and PREG docked to the  $\beta_3/\alpha_1$  intersubunit site, their 3-hydroxy, 18 and 19 methyl and methyl ketone groups all assume overlapping positions, consistent with their similar potency and efficacy as GABA<sub>A</sub> receptor PAMs. *ent*-PREG docks with similar energy in either orientation #1 or #2 (Table 1). A comparison of *ent*-PREG and PREG in their lowest energy poses (both orientation #1) shows that their methyl ketones and 18 and 19 methyl groups roughly align and their 3-hydroxy groups both point toward  $\alpha_1$ -TM1, consistent with the minimal enantioselectivity of PREG (Figure 3b). In contrast to the other neurosteroids, the energetically preferred pose of *ent*-ALLO is in orientation #2. In this pose, the C18 and C19 methyl groups are aligned with the ALLO methyl groups, but the 3-hydroxy group is not positioned to form a hydrogen bond with either Q242 or W246 (Figure 3c). *ent*-ALLO docking in orientation #1 is less energetically favorable (Table 1). A comparison of ALLO to *ent*-ALLO binding in orientation #1 shows that the methyl groups of the two steroids point in almost opposite directions and the *ent*-ALLO 3-hydroxy group is not proximal to Q242. (Figure 3d).

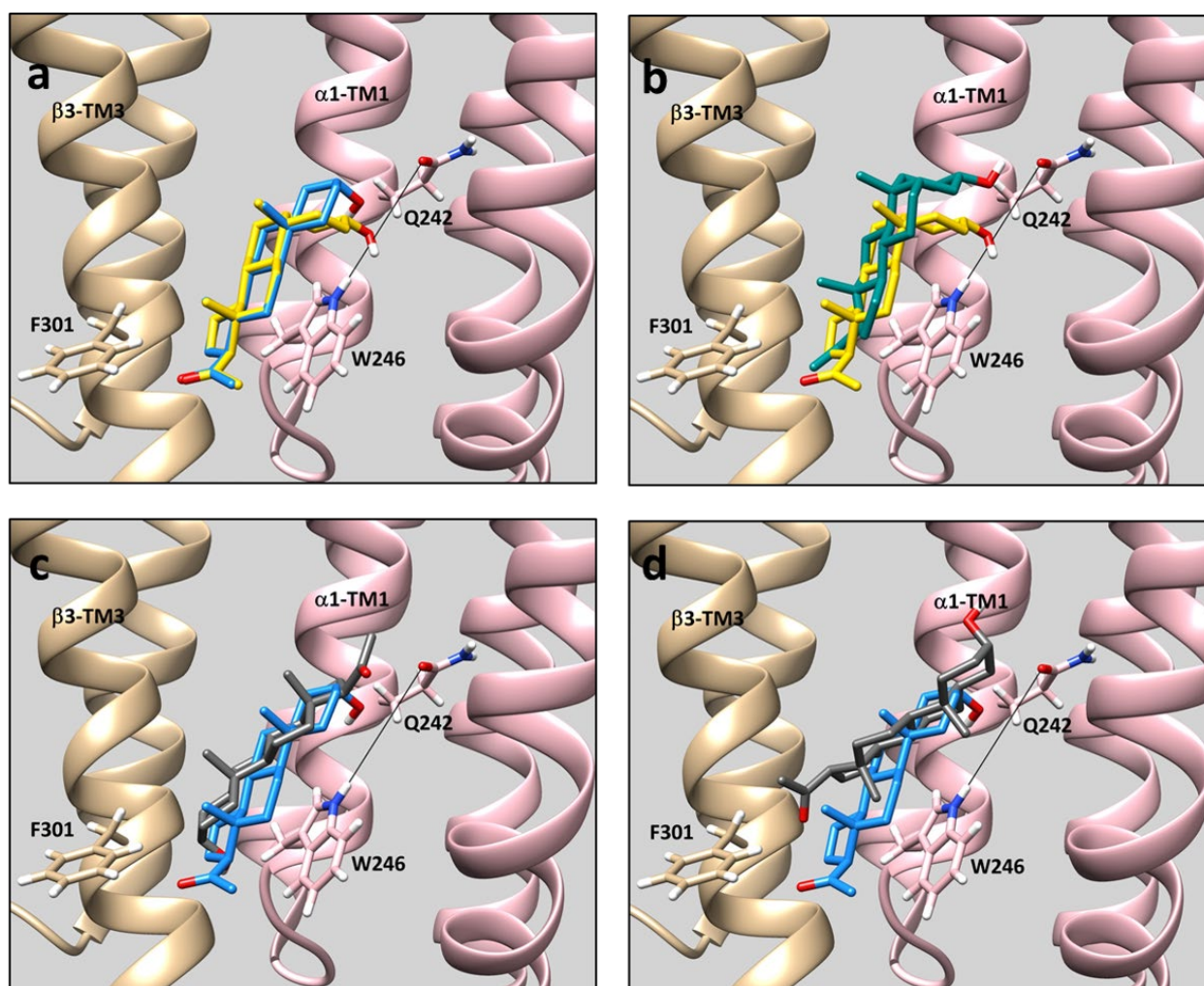


**Figure 3.** Comparison of steroid docking poses in the  $\beta_3/\alpha_1$  intersubunit binding site of the GABA<sub>A</sub> receptor using the cryo-EM structure (PDB 6HUO) of a  $\alpha_1\beta_3\gamma_2$  GABA<sub>A</sub> receptor. The  $\beta_3$  subunit is shown in tan and the  $\alpha_1$  subunit in pink. Sidechains of the  $\alpha_1$ (Q242) and  $\alpha_1$ (W246) residues are shown connected by a line indicating the axis of the coordinated hydrogen bonds formed by these two residues with the steroid 3-hydroxy group. The side chain of  $\beta_3$ (F301), a residue known to line the steroid binding site is also shown. The structure of ALLO is shown in blue, *ent*-ALLO in grey, PREG in yellow and *ent*-PREG in green. (a) ALLO and PREG in their lowest energy poses. (Both steroids are in Orientation #1 (See Table 1)). The steroid rings, methyl groups and methyl ketones are aligned with the 3-hydroxy groups of both steroids positioned to form hydrogen bonds with Q242 and W246. (b) PREG and *ent*-PREG in their lowest energy poses. (Both steroids are in Orientation #1.) The methyl groups and methyl ketones of both steroids are similarly oriented and the 3-hydroxy groups of both steroids are positioned to hydrogen bond with Q242. (c) ALLO and *ent*-ALLO in their lowest energy poses. While the methyl groups of the two steroids are similarly positioned, the 3-hydroxyl group of *ent*-ALLO is oriented 180° from ALLO and points to F301; it is thus not positioned to form a hydrogen bond with Q242 or W246. (ALLO is in Orientation #1, whereas *ent*-ALLO is in Orientation #2.) (d) Comparison of ALLO (lowest energy pose) with *ent*-ALLO in the lowest energy pose in which the 3-hydroxy group points toward the  $\alpha_1$  subunit. (Both steroids are in Orientation #1.) The methyl groups of the two steroids are oriented in opposite directions and the 3-hydroxy group of *ent*-ALLO is pointing away from Q242. The absence of a hydrogen bond and the malposition of the methyl groups likely makes this an energetically unfavorable pose for *ent*-ALLO binding. The Vina docking scores for the steroids in each pose are shown in Table 1.

**Table 1.** Lowest energy Vina scores for docking of steroids in the  $\beta_3/\alpha_1$  intersubunit neurosteroid binding pocket of the GABA<sub>A</sub> receptor using the Cryo-EM structure of an  $\alpha_1\beta_3\gamma_2$  receptor (PDB: 6HUO). Orientation 1 refers to poses in which the 3-hydroxy group of the steroid is oriented toward  $\alpha_1$ (Q242) and the methyl ketone is oriented toward  $\beta_3$ (F301). Orientation 2 refers to poses in which the 3-hydroxy group is oriented toward  $\beta_3$ (F301) and the methyl ketone is oriented toward  $\alpha_1$ (Q242). Docking was performed using AutoDock Vina embedded in UCSF Chimera ver. 1.16.

Ligand	Docking Score (kcal/mol.)	
	Orientation 1	Orientation 2
ALLO	−8.3	−7.4
<i>ent</i> -ALLO	−7.3	−7.9
PREG	−8.3	−7.5
<i>ent</i> -PREG	−7.4	−7.3

### 3.4. Steroid Binding to the $\alpha_1$ and $\beta_3$ Intrasubunit Site on $\alpha_1\beta_3$ GABA<sub>A</sub> Receptors

While electrophysiological and mutational data indicate that the PAM effects of ALLO, *ent*-ALLO, PREG and *ent*-PREG are largely mediated by the  $\beta_3/\alpha_1$  intersubunit site, neurosteroids also bind to and act through  $\beta_3$  and  $\alpha_1$  intrasubunit sites [9,16]. To examine binding to the  $\beta_3$  intrasubunit site, we measured the ability of the ALLO and PREG enantiomeric pairs to prevent photolabeling by the ALLO-analogue photolabeling reagent, KK123 (Figure 2A). KK123 labels residue Y442 on the  $\beta_3$ -TM4 peptide in the  $\beta_3$  intrasubunit site (Figure 2B and Figure S1) [9]. KK123 (3  $\mu$ M) photolabeling in the  $\beta_3$  intrasubunit site was completely prevented by 30  $\mu$ M ALLO, *ent*-ALLO, PREG, and *ent*-PREG ( $p < 0.001$ , vs. control, respectively,  $n = 3$  per group) (Figure 2D). KK123 also labeled the  $\alpha_1$  intrasubunit site at residue Y415 on  $\alpha_1$ -TM4 [9], but the efficiency of labeling was too low to reliably measure competitive prevention of photolabeling.

Since we could not measure *ent*-ALLO binding to the  $\alpha_1$  intrasubunit site using competitive prevention of photolabeling, we took an alternative approach of labeling GABA<sub>A</sub> receptors with KK152, the enantiomer of KK123 (Figure 4A), and identifying the adducted residue using mass spectrometry. KK152 shows minimal GABA<sub>A</sub> receptor PAM activity, whereas KK123 is a strong GABA potentiator mimicking the effects of the ALLO/*ent*-ALLO enantiomeric pair [23]. We labeled HEK cell membranes containing  $\alpha_{1\text{His}}/\text{FLAG}\beta_3$  GABA<sub>A</sub> receptors with 30  $\mu$ M KK152, purified the receptors using FLAG-agarose affinity chromatography, and analyzed the protein sequence using middle-down mass spectrometry. Peptides for each of the 8 TMDs (TMD1–4 for  $\alpha_1$  and  $\beta_3$ ) were identified with 100% peptide-level coverage (Supplementary Figure S2). To identify KK152-labeled peptides, we searched for TMD peptides with the precise add weight of KK152 and with a chromatographic retention time slightly longer than the unmodified peptide. This latter criterion reflects the fact that addition of a steroid increases the hydrophobicity of TMD peptides, shifting their reverse-phase chromatographic retention to later times. Using these criteria, MS1 features corresponding to an  $\alpha_1$ -TM4 peptide with a single KK152 adduct were identified. Extracted ion chromatograms of unlabeled and KK152-labeled  $\alpha_1$  subunit TM4 peptides are shown in Figure 4B. The blue peak represents the unlabeled peptide with a retention time of 105.9 min and the red peak is the KK152-labeled peptide with a retention time of 108.5 min. The  $\alpha_1$ -TM4 KK152 adducted peptide was identified as  $^{398}\text{I}^{\text{A}}\text{FPLLFGIFNLVYWATYLNREPQLK}^{423} + \text{KK152}$  ( $m/z = 1167.0008$ ,  $z = 3$ ). A fragmentation ion spectrum of this peptide identified Tyr415 as the site of KK152 adduction (Figure 4C,D). This is the same residue that is labeled by KK123. While this demonstrates binding of KK152 to the  $\alpha_1$  intrasubunit site, the photolabeling efficiency observed with 3  $\mu$ M KK152 (maximum concentration for competition studies) was inadequate to examine competitive prevention of photolabeling.



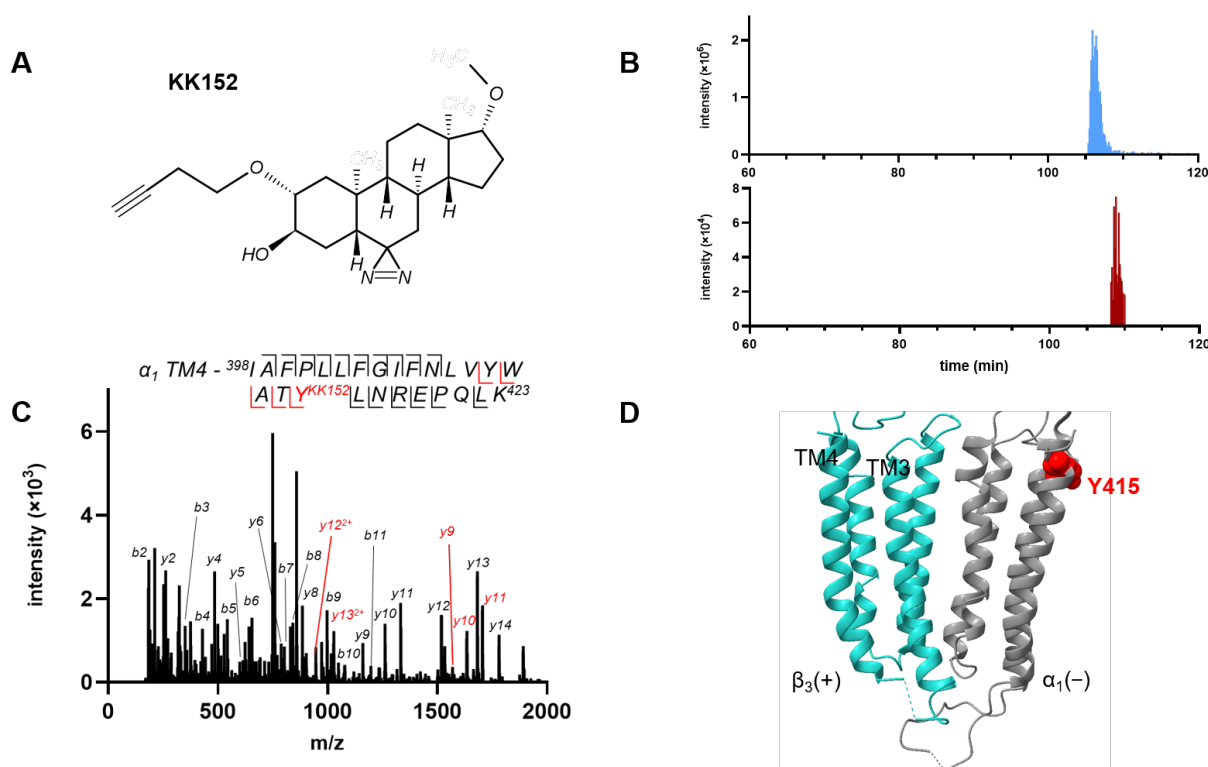


**Figure 4.** Photolabeling of  $\alpha_1\beta_3$  GABA<sub>A</sub> receptors by KK152 (the enantiomer of KK123). **(A)** The structure of KK152. **(B)** Extracted ion chromatograms from mass spectrometric analysis illustrating the labeling of  $\alpha_1$ -TM4 peptide in  $\alpha_1\beta_3$  GABA<sub>A</sub> receptors by KK152. The y-axis shows the intensity of the unlabeled TM4 peptide (top panel) and the KK152-labeled TM4 peptide (bottom panel). The x-axis shows the chromatographic retention time of the unlabeled TM4 peptide (blue, 105.9 min) and the KK152-labeled TM4 peptide (red, 108.5 min) illustrating that the increased hydrophobicity of the labeled peptide lengthens retention time on reversed phase chromatography. **(C)** HCD fragmentation spectrum of the  $\alpha_1$  subunit TM4 tryptic peptide photolabeled by 30  $\mu$ M KK152. Red and black indicate fragment ions that do or do not contain KK152, respectively. The peptide sequence shows that the y-ion series of fragment ions contains diagnostic peptides indicating labeling of residue  $\alpha_1$  (Y415). **(D)** Structure of the  $\alpha_1\beta_3$  GABA<sub>A</sub> receptor showing the location of Y415, the residue labeled by KK152 at the exoplasmic end of  $\alpha_1$  TM4. The  $\alpha_1$  subunit is shown in grey and the  $\beta_3$  subunit in turquoise.

#### 4. Discussion

In this study we determined the molecular basis for the enantioselective action of ALLO and the relative lack of enantioselectivity of PREG as GABA<sub>A</sub>-PAMs. The data show that the enantioselectivity of ALLO is based on differential binding affinity and efficacy of the ALLO enantiomers in the  $\beta_3/\alpha_1$  intersubunit neurosteroid binding site on GABA<sub>A</sub> receptors. The evidence in support of this conclusion includes: (1) Electrophysiological concentration-response data showing that *ent*-ALLO is at least 20-fold less potent and less efficacious than ALLO as a GABA<sub>A</sub>-PAM; (2) Mutagenesis data showing that the modest PAM effects of *ent*-ALLO are prevented by a mutation ( $\alpha_1$ (Q242L)) known to prevent neurosteroid action in the  $\beta_3/\alpha_1$  intersubunit site [8]; and (3) Photolabeling/mass spectrometry results showing that both *ent*-ALLO and ALLO bind to the  $\alpha_1$  and  $\beta_3$  intrasubunit neurosteroid binding sites, but that *ent*-ALLO binds with very low affinity to the  $\beta_3/\alpha_1$  intersubunit site.

These data also explain the lack of diastereoselectivity between ALLO and its 5 $\beta$ -epimer PREG and the minimal enantioselectivity of PREG. No significant differences in binding to the intrasubunit or intersubunit neurosteroid binding sites were observed between ALLO, PREG and *ent*-PREG. All three compounds had equal efficacy as GABA-PAMs and their

PAM effects were prevented by the  $\alpha_1$ (Q242L) mutation, indicating that their PAM actions are largely mediated by binding to the intersubunit site.

Rigid body docking provides some insight into the complex pattern of diastereoselective and enantioselective binding and GABA<sub>A</sub>-PAM activity of the ALLO and PREG enantiomeric pairs. Despite the marked difference in configuration between ALLO and PREG (*cis* vs. *trans* A,B-ring fusion), their energetically preferred poses in the intersubunit site are closely aligned, with their 18 and 19 methyl (“rough surface”) and 17-methyl ketone groups superimposed and their 3-hydroxy groups positioned to form coordinated hydrogen bonds with  $\alpha_1$ (Q242) and  $\alpha_1$ (W246) (Figure 3a) [12]. This explains their lack of diastereoselective GABA<sub>A</sub>-PAM activity. *ent*-PREG, in its preferred pose, is rotated 180° on its short axis in comparison to PREG. In this pose the methyl groups and methyl ketone groups of *ent*-PREG and PREG are aligned and the 3-hydroxy group of *ent*-PREG is positioned to form a hydrogen bond with  $\alpha_1$ (Q242) (Figure 3b). These poses explain the modest degree of enantioselectivity of PREG as a GABA<sub>A</sub>-PAM. In contrast, *ent*-ALLO in its lowest energy pose, is rotated 180° on its long axis in comparison to ALLO, PREG and *ent*-PREG. While the methyl groups of ALLO and *ent*-ALLO align in this pose, the *ent*-ALLO 3-hydroxy group is proximal to  $\beta_3$ (F301), and is not positioned to form a hydrogen bond with either  $\alpha_1$ (Q242) or  $\alpha_1$ (W246) (Figure 3c). The lowest energy pose in which the 3-hydroxyl group of *ent*-ALLO points toward  $\alpha_1$ (Q242) (Figure 3d) is energetically unfavorable both because the 3-hydroxy group is not positioned to form a hydrogen bond with Q242 and/or W246 and because the 18 and 19 methyl groups point toward W246, potentially interfering with steroid ring-tryptophan stacking interactions.

While docking studies provide inference about binding, the  $\beta_3$ - $\alpha_1$  intersubunit site is on the protein surface and bound neurosteroids interact with both protein and surrounding membrane lipid. The contribution of hydrogen binding to total binding energy is likely to be greater in the nonpolar environment of the lipid membrane than in the *in vacuo* conditions modeled in docking algorithms [29]. As such, the absence of *ent*-ALLO hydrogen bonding to Q242 or W246 may reduce binding energy more than is predicted by docking studies. It is also not clear if *ent*-ALLO dominantly binds in orientation #1 (Figure 3d), orientation #2 (Figure 3c) or both. However, the absence of hydrogen bonding in either orientation is likely to contribute to low affinity and low efficacy.

The finding that *ent*-ALLO binds in the opposite orientation from ALLO in the  $\beta_3$ - $\alpha_1$  intersubunit site is consistent with our previous observation that mutations in the intersubunit binding site that interfere with neurosteroid action change steroid orientation in the binding site. In a wild-type ELIC- $\alpha_1$  GABA<sub>A</sub> chimeric receptor, KK200 (photolabeling moiety on the D-ring) labeled residue Y309 at the bottom of TM3, whereas in receptors with the Q242L or W246L mutations, it labeled residue F298 in the middle of the TM3 helix [30]. These data indicate that the 3-hydroxy group on the steroid A-ring is oriented to the center of the transmembrane domain in wild-type receptors, but to the cytoplasmic end of the transmembrane helices in the mutant receptors. Elimination of a hydrogen bonding interaction between the 3-hydroxy group of a neurosteroid and the Q242 and/or W246 residues, either because of mutation or steroid structure, may favor a steroid orientation in which the 3-hydroxyl group points to the cytoplasmic interface with the membrane, similar to its preferred orientation in a lipid bilayer [31].

The results of this study elucidate the molecular interactions underlying ALLO enantioselectivity, but may also have some practical pharmacological implications. ALLO interacts with three binding sites on  $\alpha_1\beta_3$  GABA<sub>A</sub> receptors, all of which mediate allosteric effects on channel function [9,15,18]. The preferential interaction of *ent*-ALLO with the intrasubunit sites suggests its potential utility as a site-selective ligand or as a scaffold for a site-selective neurosteroid ligand.

The enantiomers of ALLO were originally used to demonstrate that PAM neurosteroids act by binding to specific sites on the GABA<sub>A</sub> receptor, rather than by perturbing the lipid membrane milieu in which the receptor resides [5]. Consistent with this idea, our data demonstrate differential binding of ALLO and *ent*-ALLO to the same site on a GABA<sub>A</sub>



receptor. However, our data for PREG and *ent*-PREG show that an enantiomeric pair of ligands can also bind to the same site with near identical affinity and efficacy. Thus, the presence of enantioselectivity supports a direct protein binding interaction, but its absence does not refute it. There is an old pharmacologic “rule” (Pfeiffer’s Rule) that states that the ratio (eudismic ratio) of the potency of a ligand (eutomer) to its less active enantiomer (distomer) is proportional to the potency of the eutomer [32]. ALLO and PREG bind with similar affinity to the  $\beta_3/\alpha_1$  intersubunit site on GABA<sub>A</sub> receptors, producing a PAM effect of similar magnitude. However, *ent*-ALLO binds to the intersubunit site with much lower affinity than *ent*-PREG, producing a markedly smaller PAM effect. The difference in eudismic ratio between the ALLO and PREG enantiomeric pairs clearly contradicts Pfeiffer’s rule [33].

**Supplementary Materials:** The following are available online at <https://www.mdpi.com/article/10.3390/biom13020341/s1>, Figure S1: Fragmentation ion spectra of KK200 and KK123 labeled peptides. Figure S2: Mass spectrometric sequence coverage of  $\alpha_1$  and  $\beta_3$  GABA<sub>A</sub> receptor subunits.

**Author Contributions:** Conceptualization, A.S.E., H.T. and D.F.C.; methodology, Z.C., G.A. and S.M.C.; formal analysis, A.S.E., G.A. and S.M.C.; investigation, H.T., L.W., F.A., J.B., A.L.G. and S.R.P.; resources, A.S.E. and D.F.C.; writing—original draft, A.S.E.; writing—review and editing, G.A., D.F.C., H.T., S.M.C. and J.B.; supervision, A.S.E. and G.A.; project administration, A.S.E.; funding acquisition, A.S.E. and G.A. All authors have read and agreed to the published version of the manuscript.

**Funding:** This research was funded by NIGMS-RO11108799 (A.S.E.) and NIMH-P50MH122379 (A.S.E., D.F.C.) and NIGMS-R35 GM140947 (G.A.) and the Taylor Institute for Innovative Psychiatry (A.S.E., Z.W.C., D.F.C., G.A.).

**Institutional Review Board Statement:** Not applicable.

**Informed Consent Statement:** Not applicable.

**Data Availability Statement:** The data presented in this study are available on request from the corresponding author.

**Conflicts of Interest:** The authors declare no conflict of interest.

## References

1. Dickinson, R.; Franks, N.P.; Lieb, W.R. Can the Stereoselective Effects of the Anesthetic Isoflurane Be Accounted for by Lipid Solubility? *Biophys. J.* **1994**, *66*, 2019–2023. [[CrossRef](#)]
2. Franks, N.P.; Lieb, W.R. Stereospecific Effects of Inhalational General Anesthetic Optical Isomers on Nerve Ion Channels. *Science* **1991**, *254*, 427–430. [[CrossRef](#)]
3. Alakoskela, J.-M.; Covey, D.F.; Kinnunen, P.K.J. Lack of Enantiomeric Specificity in the Effects of Anesthetic Steroids on Lipid Bilayers. *Biochim. Biophys. Acta* **2007**, *1768*, 131–145. [[CrossRef](#)] [[PubMed](#)]
4. Tomlin, S.L.; Jenkins, A.; Lieb, W.R.; Franks, N.P. Stereoselective Effects of Etomidate Optical Isomers on Gamma-Aminobutyric Acid Type A Receptors and Animals. *Anesthesiology* **1998**, *88*, 708–717. [[CrossRef](#)]
5. Wittmer, L.L.; Hu, Y.; Kalkbrenner, M.; Evers, A.S.; Zorumski, C.F.; Covey, D.F. Enantioselectivity of Steroid-Induced Gamma-Aminobutyric Acid A Receptor Modulation and Anesthesia. *Mol. Pharmacol.* **1996**, *50*, 1581–1586.
6. Li, W.; Covey, D.F.; Alakoskela, J.-M.; Kinnunen, P.K.J.; Steinbach, J.H. Enantiomers of Neuroactive Steroids Support a Specific Interaction with the GABA-C Receptor as the Mechanism of Steroid Action. *Mol. Pharmacol.* **2006**, *69*, 1779–1782. [[CrossRef](#)] [[PubMed](#)]
7. Covey, D.F.; Nathan, D.; Kalkbrenner, M.; Nilsson, K.R.; Hu, Y.; Zorumski, C.F.; Evers, A.S. Enantioselectivity of Pregnanolone-Induced Gamma-Aminobutyric Acid(A) Receptor Modulation and Anesthesia. *J. Pharmacol. Exp. Ther.* **2000**, *293*, 1009–1016.
8. Hosie, A.M.; Wilkins, M.E.; da Silva, H.M.A.; Smart, T.G. Endogenous Neurosteroids Regulate GABA<sub>A</sub> Receptors through Two Discrete Transmembrane Sites. *Nature* **2006**, *444*, 486–489. [[CrossRef](#)]
9. Chen, Z.-W.; Bracamontes, J.R.; Budelier, M.M.; Germann, A.L.; Shin, D.J.; Kathiresan, K.; Qian, M.-X.; Manion, B.; Cheng, W.W.L.; Reichert, D.E.; et al. Multiple Functional Neurosteroid Binding Sites on GABA<sub>A</sub> Receptors. *PLoS Biol.* **2019**, *17*, e3000157. [[CrossRef](#)] [[PubMed](#)]
10. Chen, Z.-W.; Manion, B.; Townsend, R.R.; Reichert, D.E.; Covey, D.F.; Steinbach, J.H.; Sieghart, W.; Fuchs, K.; Evers, A.S. Neurosteroid Analog Photolabeling of a Site in the Third Transmembrane Domain of the B3 Subunit of the GABA(A) Receptor. *Mol. Pharmacol.* **2012**, *82*, 408–419. [[CrossRef](#)]
11. Jayakar, S.S.; Chiara, D.C.; Zhou, X.; Wu, B.; Bruzik, K.S.; Miller, K.W.; Cohen, J.B. Photoaffinity Labeling Identifies an Intersubunit Steroid-Binding Site in Heteromeric GABA Type A (GABA<sub>A</sub>) Receptors. *J. Biol. Chem.* **2020**, *295*, 11495–11512. [[CrossRef](#)]

12. Miller, P.S.; Scott, S.; Masiulis, S.; De Colibus, L.; Pardon, E.; Steyaert, J.; Aricescu, A.R. Structural Basis for GABAA Receptor Potentiation by Neurosteroids. *Nat. Struct. Mol. Biol.* **2017**, *24*, 986–992. [[CrossRef](#)]
13. Lavery, D.; Thomas, P.; Field, M.; Andersen, O.J.; Gold, M.G.; Biggin, P.C.; Gielen, M.; Smart, T.G. Crystal Structures of a GABAA-Receptor Chimera Reveal New Endogenous Neurosteroid-Binding Sites. *Nat. Struct. Mol. Biol.* **2017**, *24*, 977–985. [[CrossRef](#)] [[PubMed](#)]
14. Chen, Q.; Wells, M.M.; Arjunan, P.; Tillman, T.S.; Cohen, A.E.; Xu, Y.; Tang, P. Structural Basis of Neurosteroid Anesthetic Action on GABAA Receptors. *Nat. Commun.* **2018**, *9*, 3972. [[CrossRef](#)] [[PubMed](#)]
15. Wang, L.; Covey, D.F.; Akk, G.; Evers, A.S. Neurosteroid Modulation of GABAA Receptor Function by Independent Action at Multiple Specific Binding Sites. *Curr. Neuropharmacol.* **2022**, *20*, 886–890. [[CrossRef](#)]
16. Germann, A.L.; Pierce, S.R.; Tateiwa, H.; Sugasawa, Y.; Reichert, D.E.; Evers, A.S.; Steinbach, J.H.; Akk, G. Intrastereoisomer and Intersubunit Steroid Binding Sites Independently and Additively Mediate  $\text{A}\beta_2\gamma_2\text{L}$  GABAA Receptor Potentiation by the Endogenous Neurosteroid Allopregnanolone. *Mol. Pharmacol.* **2021**, *100*, 19–31. [[CrossRef](#)] [[PubMed](#)]
17. Akk, G.; Li, P.; Bracamontes, J.; Reichert, D.E.; Covey, D.F.; Steinbach, J.H. Mutations of the GABA-A Receptor Alpha1 Subunit M1 Domain Reveal Unexpected Complexity for Modulation by Neuroactive Steroids. *Mol. Pharmacol.* **2008**, *74*, 614–627. [[CrossRef](#)]
18. Sugasawa, Y.; Cheng, W.W.; Bracamontes, J.R.; Chen, Z.-W.; Wang, L.; Germann, A.L.; Pierce, S.R.; Senneff, T.C.; Krishnan, K.; Reichert, D.E.; et al. Site-Specific Effects of Neurosteroids on GABAA Receptor Activation and Desensitization. *Elife* **2020**, *9*, e55331. [[CrossRef](#)]
19. Steinbach, J.H.; Akk, G. Applying the Monod-Wyman-Changeux Allosteric Activation Model to Pseudo-Steady-State Responses from GABAA Receptors. *Mol. Pharmacol.* **2019**, *95*, 106–119. [[CrossRef](#)]
20. Forman, S.A. Monod-Wyman-Changeux Allosteric Mechanisms of Action and the Pharmacology of Etomidate. *Curr. Opin. Anaesthesiol.* **2012**, *25*, 411–418. [[CrossRef](#)]
21. Akk, G.; Germann, A.L.; Sugasawa, Y.; Pierce, S.R.; Evers, A.S.; Steinbach, J.H. Enhancement of Muscimol Binding and Gating by Allosteric Modulators of the GABAA Receptor: Relating Occupancy to State Functions. *Mol. Pharmacol.* **2020**, *98*, 303–313. [[CrossRef](#)]
22. Cheng, W.W.L.; Chen, Z.-W.; Bracamontes, J.R.; Budelier, M.M.; Krishnan, K.; Shin, D.J.; Wang, C.; Jiang, X.; Covey, D.F.; Akk, G.; et al. Mapping Two Neurosteroid-Modulatory Sites in the Prototypic Pentameric Ligand-Gated Ion Channel GLIC. *J. Biol. Chem.* **2018**, *293*, 3013–3027. [[CrossRef](#)] [[PubMed](#)]
23. Jiang, X.; Shu, H.-J.; Krishnan, K.; Qian, M.; Taylor, A.A.; Covey, D.F.; Zorumski, C.F.; Mennerick, S. A Clickable Neurosteroid Photolabel Reveals Selective Golgi Compartmentalization with Preferential Impact on Proximal Inhibition. *Neuropharmacology* **2016**, *108*, 193–206. [[CrossRef](#)] [[PubMed](#)]
24. Darbandi-Tonkabon, R.; Hastings, W.R.; Zeng, C.-M.; Akk, G.; Manion, B.D.; Bracamontes, J.R.; Steinbach, J.H.; Mennerick, S.J.; Covey, D.F.; Evers, A.S. Photoaffinity Labeling with a Neuroactive Steroid Analogue. *J. Biol. Chem.* **2003**, *278*, 13196–13206. [[CrossRef](#)] [[PubMed](#)]
25. Hanwell, M.D.; Curtis, D.E.; Lonie, D.C.; Vandermeersch, T.; Zurek, E.; Hutchison, G.R. Avogadro: An Advanced Semantic Chemical Editor, Visualization, and Analysis Platform. *J. Cheminform.* **2012**, *4*, 17. [[CrossRef](#)] [[PubMed](#)]
26. Masiulis, S.; Desai, R.; Uchański, T.; Serna Martin, I.; Lavery, D.; Karia, D.; Malinauskas, T.; Zivanov, J.; Pardon, E.; Kotecha, A.; et al. GABAA Receptor Signalling Mechanisms Revealed by Structural Pharmacology. *Nature* **2019**, *565*, 454–459. [[CrossRef](#)]
27. Pettersen, E.F.; Goddard, T.D.; Huang, C.C.; Couch, G.S.; Greenblatt, D.M.; Meng, E.C.; Ferrin, T.E. UCSF Chimera—A Visualization System for Exploratory Research and Analysis. *J. Comput. Chem.* **2004**, *25*, 1605–1612. [[CrossRef](#)]
28. Trott, O.; Olson, A.J. AutoDock Vina: Improving the Speed and Accuracy of Docking with a New Scoring Function, Efficient Optimization, and Multithreading. *J. Comput. Chem.* **2010**, *31*, 455–461. [[CrossRef](#)]
29. Lee, A.G. A Database of Predicted Binding Sites for Cholesterol on Membrane Proteins, Deep in the Membrane. *Biophys. J.* **2018**, *115*, 522–532. [[CrossRef](#)]
30. Sugasawa, Y.; Bracamontes, J.R.; Krishnan, K.; Covey, D.F.; Reichert, D.E.; Akk, G.; Chen, Q.; Tang, P.; Evers, A.S.; Cheng, W.W.L. The Molecular Determinants of Neurosteroid Binding in the GABA(A) Receptor. *J. Steroid Biochem. Mol. Biol.* **2019**, *192*, 105383. [[CrossRef](#)]
31. Atkovska, K.; Klingler, J.; Oberwinkler, J.; Keller, S.; Hub, J.S. Rationalizing Steroid Interactions with Lipid Membranes: Conformations, Partitioning, and Kinetics. *ACS Cent. Sci.* **2018**, *4*, 1155–1165. [[CrossRef](#)] [[PubMed](#)]
32. Pfeiffer, C.C. Optical Isomerism and Pharmacological Action, a Generalization. *Science* **1956**, *124*, 29–31. [[CrossRef](#)] [[PubMed](#)]
33. Barlow, R. Enantiomers: How Valid Is Pfeiffer’s Rule? *Trends Pharmacol. Sci.* **1990**, *11*, 148–150. [[CrossRef](#)] [[PubMed](#)]

**Disclaimer/Publisher’s Note:** The statements, opinions and data contained in all publications are solely those of the individual author(s) and contributor(s) and not of MDPI and/or the editor(s). MDPI and/or the editor(s) disclaim responsibility for any injury to people or property resulting from any ideas, methods, instructions or products referred to in the content.